HAL
open science

The Role of Solid Friction in the Sedimentation of Strongly Attractive Colloidal Gels

Jean-Michel Condre, Christian Ligoure, Luca Cipelletti

To cite this version:

Jean-Michel Condre, Christian Ligoure, Luca Cipelletti. The Role of Solid Friction in the Sedimentation of Strongly Attractive Colloidal Gels. Journal of Statistical Mechanics: Theory and Experiment, 2007, pp.P02010. 10.1088/1742-5468/2007/02/P02010 . hal-00103848

HAL Id: hal-00103848

https://hal.science/hal-00103848v1

Submitted on 5 Oct 2006

HAL is a multi-disciplinary open access archive for the deposit and dissemination of scientific research documents, whether they are published or not. The documents may come from teaching and research institutions in France or abroad, or from public or private research centers.

L'archive ouverte pluridisciplinaire **HAL**, est destinée au dépôt et à la diffusion de documents scientifiques de niveau recherche, publiés ou non, émanant des établissements d'enseignement et de recherche français ou étrangers, des laboratoires publics ou privés.

ccsd-00103848, version 1 - 5 Oct 2006

The Role of Solid Friction in the Sedimentation of Strongly Attractive Colloidal Gels

Jean-Michel Condre, Christian Ligoure, and Luca Cipelletti§

LCVN UMR 5587, Université Montpellier II and CNRS, P. Bataillon, 34095 Montpellier, France

Abstract.

We study experimentally and theoretically the sedimentation of gels made of strongly aggregated colloidal particles, focussing on the long time behavior, when mechanical equilibrium is asymptotically reached. The asymptotic gel height is found to vary linearly with the initial height, a finding in stark contrast with a recent study on similar gels [Manley *et al.* 2005 *Phys. Rev. Lett.* **94** 218302]. We show that the asymptotic compaction results from the balance between gravity pull, network elasticity, and solid friction between the gel and the container walls. Based on these ingredients, we propose a simple model to account for the dependence of the height loss on the initial height and volume fraction. As a result of our analysis, we show that the static friction coefficient between the gel and the container walls strongly depends on volume fraction: the higher the volume fraction, the weaker the solid friction. This nonintuitive behavior is explained using simple scaling arguments.

PACS numbers: 82.70.Gg, 47.57.ef, 61.43.Hv, 83.80.Kn

Submitted to: *JSTAT*

1. Introduction

Most colloidal systems tend to aggregate, unless special care is taken to stabilize them, e.g. by designing particles with surface charges or a sterically stabilizing polymer layer that prevent them to approach too closely, where short-ranged, strong Van der Waals or hydrophobic/hydrophilic attractive interactions prevail. As a result of aggregation, ramified structures, often with a fractal morphology, are formed. For high enough particle volume fraction, φ_0, and interaction strength, these aggregates form a space-filling network which is termed a colloidal gel [1]. The fate of colloidal gels depends crucially on gravity, since the magnitude of both their elastic modulus and yield stress are generally comparable to the gravitational stress due to the mismatch between the density of the particles and that of the solvent in which they are dispersed.

Because colloidal aggregates and gels are ubiquitous in the food, drug, cosmetic and oil industry and in biological systems, a large number of works has been devoted to the sedimentation (or the creaming) of aggregated colloidal systems.

§ To whom correspondence should be addressed (lucacip@lcvn.univ-montp2.fr)

Most investigations have dealt with "weak" gels, where the interparticle attraction is comparable to $k_{\mathrm{B}}T$, the thermal energy [2, 3, 4, 5]. Experimentally, this is typically the situation encountered in systems where the attraction between the colloids is induced by the addition of smaller particles or polymers via the so-called depletion mechanism [6]. For these systems, various sedimentation regimes have been observed, ranging from "creeping" sedimentation (a linear decrease of the gel height, h, with time t) to "delayed" sedimentation ($h(t)$ is nearly constant during an initial latency time, followed by a sudden collapse of the gel and a final slow compaction of the sediment). Moreover, the sedimentation of samples with identical composition may drastically differ according to the container size and shape and in particulary depending on the initial height of the gel, h_0. This behavior can be rationalized according to whether or not stress can be transmitted through the sample over distances comparable to the container size [7, 8]. This is the case for the strongest gels, where the attractive interactions are large enough to make it likely that connecting paths along the gel network persist, in spite of the continuous breaking and reforming of particle bonds due to thermal energy.

The group of C. Allain has extensively studied stronger gels, where particle bonds are unlikely to break because of thermal energy [9, 10, 11, 12]. These gels, however, are still weak enough to experience extensive restructuring due to the gravitational stress. For the most diluted samples, the very formation of a gel is prevented, because clusters grow more slowly than in concentrated samples and they sediment before getting a chance to form a system-spanning network. By contrast, Manley and coworkers have studied "strong" gels made of silica particles where neither thermal energy nor gravitational stress are large enough to cause significant restructuring of the network [13]. They find that $h(t)$ relaxes exponentially towards an asymptotic height h_∞ and propose that this behavior results from the competition between network elasticity, gravitational pull, and viscous drag of the solvent through the gel pores.

In this paper, we study strongly attractive colloidal gels similar to those of Manley *et al.*, albeit at slightly smaller volume fractions. Although we observe a similar exponential evolution of $h(t)$, we find that $\Delta_\infty \equiv h_0 - h_\infty$ is proportional to the initial height, a behavior incompatible with that predicted by the model of reference [13]. The volume fraction dependence of the sedimentation is also found to deviate with respect to that postulated in [13]. We propose a more general model for the equilibrium behavior of strongly attractive colloidal gels: in addition to network elasticity and gravitational stress, our model introduces a term describing the solid friction between the gel and the cell walls, using a formalism similar to that first developed by Janssen for granular materials [14]. The model accounts for all our experimental observations and allows us to estimate the static friction coefficient, μ_s, between the gel and the walls. Quite surprisingly, we find that μ_s *decreases* with increasing volume fraction. We propose a simple scaling argument to show that this counterintuitive behavior is due to the fractal nature of the aggregates forming the gel.

2. Materials and methods

We use aqueous dispersions of charge-stabilized silica spheres (Ludox TM-50) with radius $a \approx 11$ nm. Aggregation is induced by mixing equal volumes of a particle suspension and a NaCl solution to a final salt concentration of 2M and final particle volume fractions φ_0 ranging from 2.5×10^{-3} to 10^{-2}. At this ionic strength, electrostatic repulsion becomes negligible and the particles experience short-ranged,

strong van der Waals interactions, leading to the formation of aggregates in the diffusion limited cluster aggregation (DLCA) regime [15]. The bond energy is of the order of several tens of $k_{\mathrm{B}}T$, making thermally activated rearrangements extremely unlikely. The aggregates have a fractal dimension $d_f \approx 1.9$; during aggregation their typical size increases until they form a space-filling network. When this gelled structure is formed, the aggregates have a size distribution peaked about an average cluster size $\xi \approx a\varphi_0^{1/(d_f-3)}$ [16]. The gelation time can be calculated within the DLCA model: for our gels it is less than a few seconds [17].

The gels are viscoelastic materials: oscillatory strain measurements show that over a large range of frequencies (typically 10^{-2} rad/sec $< \omega <$ 10 rad/sec) the storage modulus G' is nearly frequent-independent and about one order of magnitude larger than the loss modulus G" [20, 21]. Due to the fractal morphology of the gels, G' increases very strongly with volume fraction: $G' \propto \varphi_0^{\nu}$ where $\nu \approx 3.6 - 4.0$ [18, 19, 20, 21]. Moreover, the gels are able to sustain large shear strains up to about 10% before the network is significantly altered and linear elasticity fails [20]. Applying larger strains leads initially to strain hardening, but eventually results in the disruption of the gels, although gel breaking may not occur instantaneously [20, 13].

The particle density is 2.35 g/cm^3, while that of the solvent is 1.15 g/cm^3 (due to the high salt concentration). The density mismatch, $\Delta\rho = 1.2$ g/cm^3, is large enough to make the gels sensitive to gravitational stress, leading to a slow compaction. Experiments are performed by directly preparing the gels in glass cylindrical cells of diameter $D = 1.7$ cm and letting them settle unperturbed. Note that contrary to the protocol of reference [10] no stirring is applied after the initial mixing of the particle and salt solutions. The gels are imaged with a CCD camera to capture the settling kinetics. We check that no cracks appear in the bulk of the gels. As observed in other experiments [3, 7], at the earliest stages of sedimentation the meniscus at the top of the suspension is emptied from the particles. Once only solvent is left in the meniscus, the gel starts settling uniformly throughout the cross section of the cell. A reasonably flat, sharp interface is observed between the highly turbid gel and the clear supernatant, allowing us to measure the time evolution of the height of the gel, $h(t)$, with an accuracy of about 5%. We define $t = 0$ as the time when the meniscus is emptied and the uniform settling starts. We study gels at six volume fractions: $\varphi_0 = 2.5 \times 10^{-3}$, 3×10^{-3}, 5×10^{-3}, 6×10^{-3}, 7.5×10^{-3}, and 10^{-2}. For $\varphi_0 < 2.5 \times 10^{-3}$ the gels often develop cracks and the experiments are less reproducible, while for $\varphi_0 > 10^{-2}$ the gels hardly settle, making a precise determination of $h(t)$ impossible with our apparatus. For each φ_0, we vary the initial height of the gel, h_0, in the range 0.5 cm $< h_0 <$ 5 cm.

3. Experimental results

Figure 1 shows the evolution of the gel height measured for $\varphi_0 = 0.3 \times 10^{-2}$ and various initial heights h_0. The time evolution of $h(t)$ is well fitted by a simple exponential relaxation:

$$h_0 - h(t) = \Delta_\infty \left[1 - \exp(-t/\tau)\right] \tag{1}$$

where $\Delta_\infty = |h_\infty - h_0|$ denotes the asymptotic settling and $h_\infty = h(t \to \infty)$. A similar behavior has been reported recently for the "strong" gels of reference [13]. Both the asymptotic settling and the characteristic time τ grow with the initial height of the gel; for the tallest gels ($h_0 = 4.9$ cm), τ is as large as a few hours. The same exponential relaxation, Eq. (1), describes the height evolution of all the gels that we

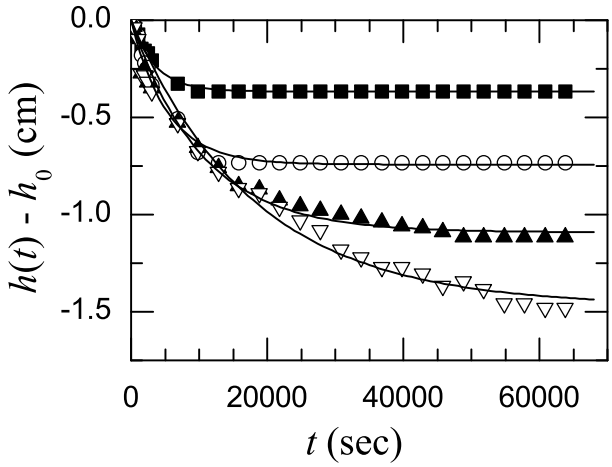

Figure 1. Time dependence of the settling of a gel with $\varphi_0 = 0.3 \times 10^{-2}$. From top to bottom, the initial height of the gel, h_0, is 1.23, 2.45, 3.68, and 4.9 cm. The lines are fits of Eq. (1) to the data.

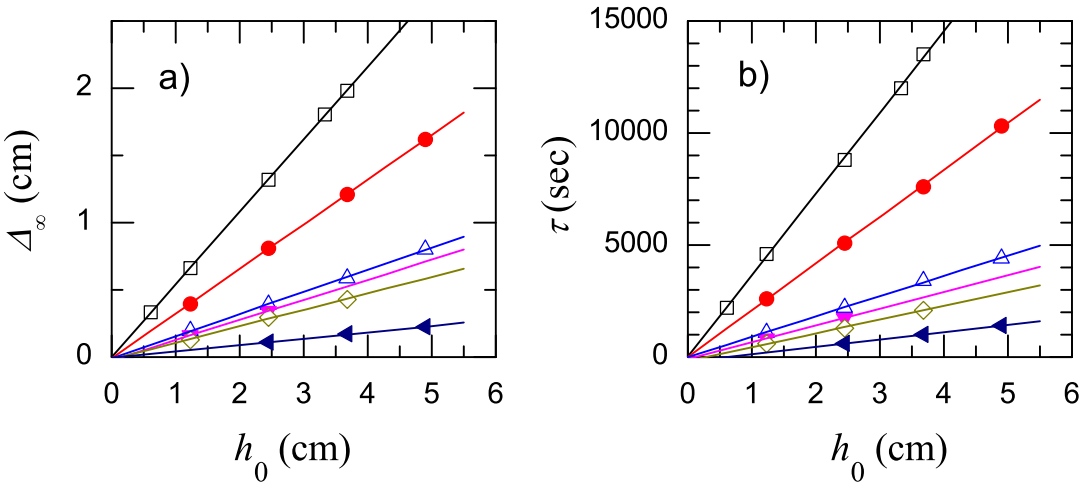

Figure 2. Asymptotic settling of the gel height Δ_∞ (a), and characteristic time τ for the sedimentation (b) as a function of the initial height h_0. From top to bottom, $\varphi_0 = 2.5 \times 10^{-3}$, 3×10^{-3}, 5×10^{-3}, 6×10^{-3}, 7.5×10^{-3}, and 1×10^{-2}. Both quantities vary linearly with h_0, as shown by the fits (straight lines).

have studied, except for some samples where fractures appeared during the settling. For fractured gels, $h(t)$ deviates from an exponential relaxation and the asymptotic settling is larger than that expected for pristine samples. In the following we analyze only data for non-fractured gels.

We plot in Fig. 2 the h_0 dependence of the asymptotic settling (a) and of the characteristic settling time (b). Remarkably, both Δ_∞ and τ vary linearly with the initial height of the gel, as shown by the lines that are fits of form $\Delta_\infty = \alpha h_0 + \alpha_1$ and $\tau = \beta h_0 + \beta_1$, respectively. As one can see in Figure 2, both α_1 and β_1 are almost

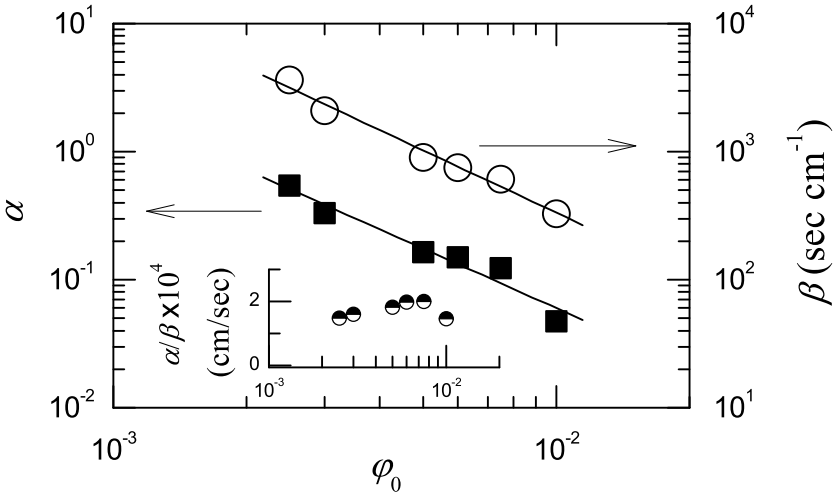

Figure 3. Left axis, solid squares: φ_0 dependence of the proportionality coefficient α between Δ_∞ and h_0 extracted from the linear fits of Fig. 2a). The line is a power law fit yielding an exponent -1.54 ± 0.17. Right axis, open circles: proportionality coefficient β between τ and h_0 extracted from the linear fits of Fig. 2b). The line is a power law fit yielding an exponent -1.62 ± 0.11. Inset: ratio α/β *vs* φ_0. Note the weak variation of α/β with volume fraction, indicating that the initial sedimentation velocity is almost constant, as discussed in the text.

zero, making the fits indistinguishable from straight lines through the origin. In fact, we find that $\beta_1 = 0$ is compatible with experimental uncertainty, while α_1 is slightly but consistently smaller than 0, a feature that will be commented further below.

For a fixed cell diameter and material, the prefactors α and β depend solely on volume fraction. Their φ_0 dependence is shown in Fig. 3 in a log-log scale. The data can be fitted reasonably well by power laws: $\alpha \sim \varphi_0^u$ and $\beta \sim \varphi_0^v$, with $u = -1.54 \pm 0.17$ and $v = -1.62 \pm 0.11$. Quite intriguingly, $u \approx v$: this indicates that for $t \to 0$ the settling velocity of the gels is nearly independent of both their height and volume fraction. Indeed, for $t << \tau$ Eq. (1) yields $|dh/dt| \approx \Delta_\infty/\tau = \alpha/\beta$, which varies weakly between 1.45×10^{-4} and 2×10^{-4} cm/sec as shown in the inset of Fig. 3.

In order to understand the behavior of our gels, we start by comparing the results presented in Figures 1–3 with previous works. C. Allain and coworkers have measured the quantity $\Omega = 1 - \Delta_\infty/h_0 = 1 - \alpha$ and found that in the so-called "friction-dominated" regime Ω is independent of the initial height h_0 [9, 10], in agreement with our observation $\Delta_\infty \approxeq \alpha h_0$. However, they find $\Omega \propto \varphi_0$, a scaling that is incompatible with the power law $\alpha \sim \varphi^{-1.62}$ shown in Figure 3, as we also check by plotting directly Ω *vs* φ_0 (data not shown). This discrepancy suggests that the physical mechanism leading to the settling of our gels is different from that of references [9, 10]. Indeed, the gels studied by Allain's group experience extensive restructuring and fractures during sedimentation [11, 12], in contrast to our gels. During sedimentation, the gel does not retain its integrity and the scaling $\Omega \propto \varphi_0$ results from the formation of a sediment composed of randomly packed aggregates issued from the gravity-induced breaking of the gel.

An exponential relaxation similar to that shown in Figure 1 has been reported for gels made of silica particles by Manley *et. al*, who studied the regime where no fractures are observed [13], similarly to our experiments. This sedimentation kinetics is interpreted as the result of the interplay between gravitational pull, network elasticity, and viscous drag of the solvent through the network pores. However, our results differ distinctly from those of reference [13] in that we find i) $\Delta_\infty \propto h_0$ rather than $\Delta_\infty \propto h_0^2$ as predicted by the model of [13], ii) $\tau \propto h_0$, as opposed to $\tau \propto h_0^2$, iii) $\tau \propto \varphi_0^{-1.62}$, rather than $\tau \propto (1-\varphi_0)$; iv) $dh/dt|_{t=0} \approx$ constant, while Manley and coworkers find $dh/dt|_{t=0} \propto \varphi^{(1-d_f)/(3-d_f)} \approx \varphi^{-0.8}$. Therefore, it is clear that in the case of our gels a fundamental physical ingredient is missing in the model of reference [13].

4. Model and comparison with the experiments

We propose that, in addition to the mechanisms listed above, solid friction between the gel and the cell walls also plays a crucial role in the settling of our samples. A hint of the importance of solid friction is provided by the observation that both Δ_∞ and τ are modified by using plexiglas cells rather than glass cells [22]. Moreover, the importance of solid friction is consistent with the arguments of reference [8], where it was argued that, for gels with strong interparticle interactions, the characteristic length over which stress can be propagated exceeds the container dimensions. Accordingly, "strong" gels such as those studied here should feel the influence of the cell walls. Solid friction is particularly appealing since it provides a simple physical mechanism to explain the linear scaling of Δ_∞ with initial height h_0, as shown by the following qualitative argument. Solid friction screens the gravitational load acting on any given cross sectional plane Σ in the gel: because part of the weight of the gel column laying above Σ is sustained by the walls, it is as if in Σ the gel experienced only the weight of a column segment of effective height L, shorter than the whole column. One can then imagine to divide a gel of height h_0 into segments of height L: under gravitational stress, each segment is compressed by the same amount, regardless of the number of segments that compose the gel. Therefore, the total compression is simply proportional to the number of segments contained in the gel, i.e. $\Delta_\infty \propto h_0/L$.

To make this argument more quantitative, we build a model for the settling of the gels, assuming that they are elastic media that compresses under their own weight, without any restructuring, and subject to solid friction against the cell walls. The rate of compression is limited both by the viscous friction of the fluid through the network, which can be viewed as a porous medium [11, 13], and by solid friction. In the following, we will focus on the behavior for $t >> \tau$, when mechanical equilibrium is asymptotically reached and gravitational stress is counterbalanced by both the gel elasticity and solid friction; the kinetics of sedimentation will be addressed in future work. We choose the z axis along the vertical direction, with $z = 0$ the bottom of the gel and $z = h_0$ its top at time $t = 0$. Due to gravity, the gel is submitted to a uniaxial compression $p(z) = -\sigma_{zz}$ where σ_{zz} is the vertical stress.

We first recall the behavior in the absence of wall friction. Newton's law for a gel slice of thickness dz at height z yields

$$-\Delta\rho g\varphi(z)\frac{\pi D^2}{4}dz - \frac{\partial p}{\partial z}\frac{\pi D^2}{4}dz = 0\,, \tag{2}$$

where $\varphi(z)$ is the local volume fraction, D the cell diameter and g the acceleration of gravity. The first term describes the gravity pull exerted on the slice, while the second

term accounts for the elastic response of the material. The conservation of the total number of particles imposes the additional condition

$$\int_0^{h_\infty} \varphi(z)dz = \int_0^{h_0} \varphi_0 dz = h_0\varphi_0 \,, \tag{3}$$

while the boundary condition is

$$\varphi(h_\infty) = \varphi_0 \,, \tag{4}$$

since the top layer of the gel is uncompressed. If the deformation is not too large, the pressure and the volume fraction are related by the equation of state of an elastic medium in the linear regime: $p(z) = C\frac{\varphi(z)-\varphi_0}{\varphi_0}$, where the uniaxial compression modulus C is a linear combination of B, the bulk modulus, and the shear modulus: $C = B + 4G/3$. Equation (2) can be solved for $\varphi(z)$; by imposing the boundary condition, Eq. (4), one obtains the asymptotic profile:

$$\varphi(z) = \varphi_0 \exp\left[(h_\infty - z)/\lambda\right] \,, \tag{5}$$

where we have introduced $\lambda = C/(\Delta\rho g\varphi_0)$, the characteristic length over which an elastic material is deformed due to gravity (the stiffer the gel, or the weaker the density mismatch, the larger λ). By requiring that Eq. (5) satisfies particle conservation (Eq. 3), one finds $\Delta_\infty = h_0 - \lambda \ln(1 + h_0/\lambda)$. In the limit $h_0 << \lambda$, this relation simplifies to $\Delta_\infty = h_0^2/(2\lambda) + \lambda\mathcal{O}(h_0/\lambda)^3$, whose leading term coincides with the expression given in reference [13]. We estimate $G \approx 7$ Pa for our gel at $\varphi_0 = 1 \times 10^{-2}$ by extrapolating the data of ref. [21]. By assuming that the order of magnitude of C is the same as that of the shear modulus plateau, one estimates $\lambda \approx 13$ cm. [Using the full model that takes into account solid friction, we will obtain λ directly from the experimental data, finding a result consistent with this estimate, see Fig. 5 below]. Hence, $h_0 < \lambda$ in all our experiments (indeed, in most cases $h_0 << \lambda$) and a quadratic scaling of Δ_∞ with h_0 should be observed. By contrast, as recalled above, we find $\Delta_\infty \propto h_0$, indicating that gravity and elasticity alone are not sufficient to correctly describe the behavior of our samples.

Solid friction has been first modeled for a container filled with a granular material by Janssen in 1895 [14]. In the Janssen model, the pressure $p(z)$ is partially redirected in the horizontal direction leading to an horizontal stress $\sigma_{rr}(z) = Kp(z)$ with $K = \frac{B-2G/3}{B+4G/3}$ the redirection coefficient. When mechanical equilibrium is reached, the effective static friction of a slice of material of thickness dz confined in a cylinder of diameter D is oriented upward and has magnitude $\pi\mu_s DKp(z)dz$, where μ_s is the static friction coefficient between the grains and the container wall. The Janssen model predicts that, when moving from the top of the grain column downward, the pressure increases reaching exponentially a saturation value with a characteristic screening length $L = D/(4\mu_s K)$. This is very different from the case of a liquid where the pressure increases linearly with depth: the saturation is due to the fact that the cylinder wall supports part of the weight of grains: the contribution to the vertical stress on a horizontal plane Σ due to the material at a height Δz above Σ decreases as $\exp(-\Delta z/L)$. Hence, the larger the contribution of solid friction, the smaller L. The universality of the Janssen scaling for the stress saturation curve has been recently shown by Ovarlez *et al.* [23]. Moreover, the Janssen model has been generalized to dynamical situations [24].

We propose to describe the solid friction between the gels and the cell walls using Janssen's formalism. At equilibrium, Eq. (2) becomes

$$-\Delta\rho g\varphi(z)\frac{\pi D^2}{4}dz - \frac{\partial p}{\partial z}\frac{\pi D^2}{4}dz + \pi\mu_s DKp(z)dz = 0\,. \tag{6}$$

It is convenient to solve Eq. (6) for the local variation in volume fraction, $\Delta\varphi(z) = \varphi(z)-\varphi_0$, rather than directly for $\varphi(z)$. Assuming again linear elasticity and using the boundary condition (4), after some standard manipulations one finds the equilibrium concentration profile:

$$\Delta\varphi(z) = \varphi_0\frac{\ell}{\lambda}\left[1-\exp\left(\frac{z-h_\infty}{\ell}\right)\right] \tag{7}$$

where we have defined a third length ℓ related to the elastic and solid friction characteristic lengths introduced above by $1/\ell = 1/L - 1/\lambda$. Note that there are no *a priori* restrictions on the sign of ℓ; $\ell = 0$ is also possible, if the elastic and friction characteristic lengths are equal. We will show in the following that for our gels $0 < \ell < h_0$: in this case Eq. (7) predicts the concentration profile to be essentially constant, except for a segment of length a few ℓ's at the top of the gel. In general, we expect both λ and L to depend on the gel volume fraction φ_0; additionally, L may contain any deviations with respect to the usual Jannsen's law for ordinary solid materials, e.g. due to the fractal morphology of the gels. For $L \to \infty$, solid friction becomes negligible and Eq. (7) reduces to the exponential profile predicted by Eq. (5). By imposing particle conservation, Δ_∞ is found to satisfy

$$\Delta_\infty = \frac{\ell}{\lambda}\left\{h_\infty - \ell\left[1-\exp(-h_\infty/\ell)\right]\right\}\,. \tag{8}$$

Because $h_\infty = h_0 - \Delta_\infty$, this expression is an implicit equation for Δ_∞ when λ and L are known and the initial height is assigned. By contrast, Eq. (8) may be used directly to fit the experimental data, which can be easily plotted as Δ_∞ *vs* h_∞, rather than *vs* h_0 as in Fig. 2.

Various settling regimes are possible, depending on the relative values of λ, L, and h_0 (or, equivalently, h_∞). Three limiting cases are identified, according to the behavior of the argument of the exponential term in the r.h.s of Eq. (8): i) $h_\infty/\ell \to 0$, for which $\Delta_\infty \approx h_\infty^2/(2\lambda)$; ii) $h_\infty/\ell \to \infty$, for which $\Delta_\infty \approx h_\infty\ell/\lambda - \ell^2/\lambda$; iii) $h_\infty/\ell \to -\infty$, for which $\Delta_\infty \approx (\lambda^2/\ell)\exp(h_\infty/|\ell|)$. The assumption of linear elasticity that was made in deriving Eqs. (7) and (8) poses an additional constraint on the solutions for Δ_∞, since linear elasticity only applies to small deformations $\Delta_\infty \lesssim h_\infty$. We recapitulate the different settling regimes in Fig. 4, which shows schematically a "state diagram" of the solutions to Eq. (8), using as "state variables" λ/h_∞ and L/h_∞ and classifying the various zones according to the value of L relative to λ. Zone I corresponds to comparable friction and elasticity characteristic lengths ($|\lambda - L| << \lambda L/h_\infty$). In zones IIa and IIb the elastic length scale dominates over the friction length scale ($L/h_\infty << 1$ and $L/h_\infty << \lambda/h_\infty$ for IIa and $1 << L/h_\infty << \lambda/h_\infty$ for IIb). The reverse applies to zones IIIa, where $\lambda/h_\infty << 1$ and $\lambda/h_\infty << L/h_\infty$, and IIIb, for which $1 << \lambda/h_\infty << L/h_\infty$. In summary, for the $L/h_\infty > 1$ portion of zone I and for zones IIb and IIIb one finds that a quadratic law applies: $\Delta_\infty \approx h_\infty^2/(2\lambda) \approx h_0^2/(2\lambda)$. Note that this is the same expression as derived in the absence of solid friction. Hence, in these zones and to leading order solid friction has no influence on the asymptotic settling. At first sight, this result is somehow surprising for zone IIb, where $L < \lambda$ and one could have guessed that solid friction would dominate over elasticity. However,

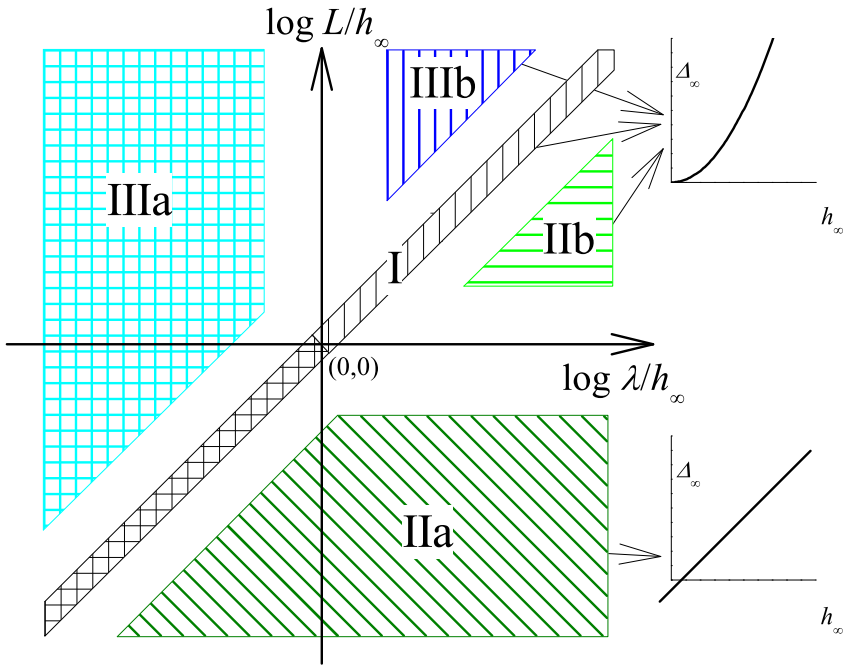

Figure 4. "State diagram" illustrating the location of the various asymptotic settling regimes discussed in the text in the $(\log \lambda/h_\infty, \log L/h_\infty)$ plane. The corresponding approximate behavior of Δ_∞ as a function of h_∞ is shown on the right. The $\lambda < h_\infty$ portion of zone I and zone IIIa should be disregarded, since they correspond to a large deformation regime that is incompatible with the assumption of linear elasticity.

our analysis shows that solid friction is negligible as long as L is much larger than the asymptotic height of the gel, regardless of the characteristic length for elasticity. In zone IIa, a linear growth is found:

$$\Delta_\infty \approx \frac{\ell}{\lambda} h_\infty - \frac{\ell^2}{\lambda}\,, \tag{9}$$

or, equivalently,

$$\Delta_\infty \approx \frac{L}{\lambda} h_0 - \frac{L^2}{\lambda - L}\,. \tag{10}$$

As one can easily check, the second term of the r.h.s. of Eq. (10) is negative and its magnitude is small compared to $h_0 L/\lambda$, yielding a nearly linear dependence of Δ_∞ on h_0, with a slightly negative $h_0 = 0$ intercept. This is precisely the behavior observed experimentally for our gels (see Fig. 2 and related discussion), strongly suggesting that our samples belong to zone IIa, where both elasticity and solid friction are present, but the contribution of the latter dominates. Finally, the $L/h_\infty < 1$ portion of zone I and zone IIIa correspond to large deformations $\Delta_\infty > h_\infty$ that are incompatible with the assumption of linear elasticity and thus should be disregarded.

To further test our model, we extract the two characteristic lengths L and λ from the height dependence of Δ_∞ and analyze both their φ_0 dependence and absolute magnitude [25]. Their volume fraction dependence is shown in Fig. 5, together with

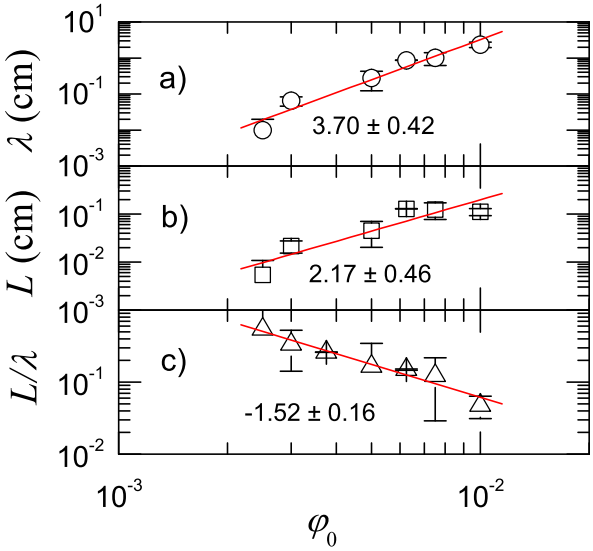

Figure 5. Volume fraction dependence of a) the elastic characteristic length λ, b) the solid friction characteristic length L, c) the ratio L/λ. The lines are power law fits to the data, whose exponent is shown in the panels. The values shown here confirm that our gels belong to zone IIa of Fig. 4, as suggested by the linear dependence of Δ_∞ *vs* h_0.

their ratio. The elastic length λ increases as $\varphi_0^{3.7\pm0.4}$, in excellent agreement with the scaling reported for the shear modulus of similar colloidal gels [18, 19, 20, 21]. Moreover, for $\varphi_0 = 10^{-2}$ we find $\lambda = 2.35$ cm, from which we calculate $C = 2.8$ Pa. This is of the same order of magnitude of, albeit somehow smaller than, the elastic shear modulus $G \approx 7$ Pa that we estimate by extrapolating the data of ref. [21] to $\varphi_0 = 10^{-2}$. The solid friction length scale L is shown in Fig. 5b). If one assumes that the relation $L = D/(4\mu_s K)$ derived for granular materials by Jennsen may apply to the gels and furthermore uses $\mu_s \approx 0.6$ and $K \lesssim 1$ as found typically for macroscopic materials, one finds $L \gtrsim 0.7$ cm, not much larger than $L \approx 0.1$ cm, the experimental value for the largest φ_0. Remarkably, however, we find that L decreases with decreasing volume fraction, strongly suggesting that the fractal nature of the gel has to be taken into account to correctly describe solid friction. Note that the variation of L with φ_0 is somehow counterintuitive, since larger values of L correspond to lesser solid friction: hence, the higher the volume fraction, the smaller the solid friction the gel experiences. We will come back to this surprising behavior in the following. The ratio L/λ is found to decrease with φ_0, a consequence of the strong increase of the elastic length scale with volume fraction. As a consistency test of the theory developed above, we check that the magnitude of λ and L are compatible with the assumption that our gels belong to zone IIa of the state diagram shown in Fig. 4 ($L << \lambda$ and $L << h_\infty$), as suggested by the linear dependence of Δ_∞ *vs* h_0. Indeed, we find that for all samples $L/\lambda < 0.54$ and $L/h_\infty < 0.12$. Moreover, the small deformation requirement is reasonably well fulfilled, since $\Delta_\infty < 0.33h_0$ for all samples, with the exception of the most diluted one, for which $\Delta_\infty = 0.54h_0$.

In order to explain the volume fraction dependence of the solid friction

characteristic length, we propose a simple argument based on the assumption that the solid friction stress between the wall and the gel is proportional to N, the number of particles per unit area in contact with the wall. During settling the gel is compressed; as a result some particles are pushed against the wall. The lower φ_0, the weaker the gel and the larger the number of particles pushed on the wall, thus leading to enhanced solid friction and smaller values of L. This argument may seem in contradiction with Amonton's law which sates that the frictional force F is proportional to the load P and is independent of the area A of the surfaces in contact [26]. However, as first observed by Coulomb, in the presence of adhesion forces F is a linear function of both load and contact area: $F = \mu P + cA$. As explained by Ringlein and Robbins [27], if the real contact area A is proportional to the load, as it is the case for elastic solids, Amonton's law follows automatically: $F = \mu_s P$ with $\mu_s = \mu + kc$. So, our assumption that the the solid friction is proportional to the number of solid particles per unit area in contact with the wall will hold if the following conditions are fulfilled: (i) the friction force between the gel and the container is mainly dominated by the adhesion of solid particles to the wall ($kc \gg \mu$); (ii) adhesive forces are negligible in determining the flattening of contact between the gel and the wall (the compaction of the gel is dominated by the gravity field). Both conditions seem realistic. When the gel is formed, the aggregates can be described as spherical blobs of volume $V \sim \xi^3$, with a negligible number of solid bonds in direct contact with the wall (zero initial friction). As the equilibrium compaction of the gel is reached, the relative variation of the blob volume, which we assume to be isotropic for simplicity, can be approximated by the first term on the r.h.s. of Eq. (10): $\Delta V/V \sim \Delta_\infty/h_0 \sim L/\lambda \sim \Delta\xi/\xi$, where the last relation applies to small deformations. For a fractal blob, the number of particles scales with blob size as $n \sim \xi^{d_f}$; therefore, the number of solid bonds per blob which will touch the wall due to a change in size $\Delta\xi$ is $\Delta n \sim \xi^{d_f-1}\Delta\xi \sim \xi^{d_f} L/\lambda$. The number of new contacts per unit area is $N \sim \Delta n/\xi^2 \sim \xi^{d_f-2} L/\lambda$; using the scaling $L/\lambda \sim \varphi_0^{-1.5}$ obtained experimentally and $\xi \sim \varphi_0^{1/(d_f-3)}$, for $d_f = 1.9$ one finally finds

$$L \sim N^{-1} \sim \varphi_0^{1.4\pm0.4}\,, \tag{11}$$

where the uncertainty in the exponent has been calculated assuming an uncertainty of 0.05 in the fractal dimension. This expression captures correctly the *decrease* of the solid friction between the wall and the gel as its volume fraction *increases*, as observed experimentally, although the exponent in Eq. (11) is lower than the measured one. In view of the large experimental uncertainties in the scaling of L (see Fig. 5) and the high sensitivity to the exact value of d_f of the exponent, the agreement seems however reasonable.

As a final remak, we note that the model proposed in this work may explain some features in previously published data on the settling of strong gels. In Fig. 1 of reference [10], Senis and Allain plot $\Omega = 1 - \Delta_\infty/h_0$ as a function of volume fraction. A power law behavior is observed, except for $\varphi_0 \gtrsim 0.01$, for which Ω tends to saturate to one, since for high-volume-fraction, stiff gels $\Delta_\infty << h_0$. One may wonder whether our model may apply to these concentrated samples. Indeed, we find that our data plotted as Ω *vs* φ_0 fit on the high volume fraction portion of the curve shown by Senis and Allain (except for an irrelevant shift factor in volume fraction, due to the difference in the physico-chemistry of the systems). This strongly suggests that for $\varphi_0 \gtrsim 0.01$ the gels of reference [10] retain their integrity and can be described by our model. Furthermore, one can see in Fig. 2 of reference [10] that for $\varphi_0 \geq 0.004$ and $h_0 \gtrsim 40$ mm $\Omega \approx$ constant similarly to our samples, implying that $\Delta_\infty \propto h_0$ and confirming

that the model proposed here applies also to the most concentrated samples of Senis and Allain. Similarly, we wonder whether some of the data by Manley and coworkers [13] may fit in the framework of our model. We recall that their system is very close to ours, the main difference being the salt that is used to induce aggregation ($MgCl_2$ at 20 mM rather than NaCl at 2 M) and the range of volume fractions investigated ($0.005 \leq \varphi_0 \leq 0.08$ in [13], as opposed to $0.0025 \leq \varphi_0 \leq 0.01$). The fact that most of their data at large volume fraction can be reproduced neglecting solid friction is consistent with our finding that L decreases with increasing φ_0, making solid friction less important for more concentrated gels. However, for the less concentrated gel and the tallest samples the h_0 dependence of τ shown in Fig. 3 of reference [13] clearly departs from the quadratic law predicted in the absence of solid friction. If a similar deviation was observed also for Δ_∞ *vs* h_0, this would suggest that for their most diluted and tallest samples solid friction does indeed play a role.

5. Conclusions

We have investigated the settling of rather diluted colloidal gels made of strongly bound silica particles, focussing on the small deformation regime where the network integrity is preserved. Contrary to previous works, we find that the asymptotic settling is incompatible with a model based only on a linear elastic response to the gravitational stress. By contrast, we are able to model our results by adding a solid friction term to the balance of forces acting on the gel. We find that solid friction plays a crucial role as long as the associated screening length L is smaller than both the gel height and the characteristic length scale λ for elastic deformation. Therefore, solid friction should matter for tall gels at moderate to small volume fractions. By contrast, solid friction is negligible when L is comparable to or larger than the gel height, regardless of the magnitude of λ. Additionally, we have shown that, due to the fractal morphology of the aggregates composing the gel, the contribution of solid friction becomes more important as the gel volume fraction decreases, a somehow surprising result.

Our work provides a more general framework for understanding and modeling the asymptotic behavior of settling gels and could easily be extended to other viscoelastic media. Future investigations should address the full kinetics of sedimentation, where we expect solid friction to play again a role, together with viscous dissipation and elastic forces.

Acknowledgments

We acknowledge financial support from CNES (grants no. 02/4800000063 and 03/4800000123), and the European Community through the "Softcomp" Network of Excellence and the Marie Curie Research and Training Network "Arrested Matter"(grant no. MRTN-CT-2003-504712). L. C. thanks the Institut Universitaire de France for supporting his research.

References

[1] Larson R G *The strructure and rheology of complex fluids* (Oxford University Press, New York, 1999).
[2] Parker A, Gunning P A, Ng K, et al. 1995 *Food Hydrocolloids* **9** 333
[3] Poon W C K, Starrs L, Meeker S P, et al. 1999 *Faraday Discuss.* **112** 143
[4] Verhaegh N A M, Asnaghi D, Lekkerkerker H N W, et al. 1997 *Physica A* **242** 104

[5] Lee M H and Furst E M 2006 *Phys. Rev.* E **74** 031401
[6] Poon W C K 2002 *J. Phys.: Condens. Matter* **14** R859
[7] Starrs L, Poon W C K, Hibberd D J, et al. 2002 *J. Phys.: Condens. Matter* **14** 2485
[8] Evans R M L and Starrs L 2002 *J. Phys.: Condens. Matter* **14** 2507
[9] Allain C, Cloitre M and Wafra M 1995 *Phys. Rev. Lett.* **74** 1478
[10] Senis D and Allain C 1997 *Phys. Rev.* E **55** 7797
[11] Senis D, Gorre-Talini L and Allain C 2001 *European Physical Journal E* **4** 59
[12] Derec C, Senis D, Talini L, et al. 2003 *Phys. Rev.* E **67** 062401
[13] Manley S, Skotheim J M, Mahadevan L, et al. 2005 *Phys. Rev. Lett.* **94** 218302
[14] Janssen 1895 *Z. Ver. Dtsch. Ing.* **39** 1045
[15] Weitz D A and Oliveria M 1984 *Phys. Rev. Lett.* **52** 1433
[16] Carpineti M and Giglio M 1992 *Phys. Rev. Lett.* **68** 3327
[17] Lin M Y, Lindsay H M, Weitz D A, et al. 1990 *J. Phys.: Condens. Matter* **2** 3093
[18] Buscall R, McGowan I J, Mills P D A, et al. 1987 *Journal of Non-Newtonian Fluid Mechanics* **24** 183
[19] Krall A H and Weitz D A 1998 *Phys. Rev. Lett.* **80** 778
[20] Gisler T and Weitz D A 1999 *Phys. Rev. Lett.* **82** 1064
[21] Manley S, Davidovitch B, Davies N R, et al. 2005 *Phys. Rev. Lett.* **95** 048302
[22] We use plexiglass cells with a 1 cm x 1 cm square cross section and height comparable to that of the glass cells.
[23] Ovarlez G, Fond C and Clement E 2003 *Phys. Rev. E* **67**
[24] Boutreux T, Raphael E and deGennes P G 1997 *Phys. Rev. E* **55** 5759
[25] Using directly Eq. (8) to fit the experimental Δ_∞ *vs* h_∞ data does not yield reliable results. This is due to the fact that the fit is sensitive essentially only to the ratio $\ell/\lambda = L/(L-\lambda)$ rather than to L and λ separately, because the first term dominates the r.h.s. of Eq. (9). To circumvent this problem, we adopt a different strategy. We use as fitting parameters ℓ/λ and λ. For a given volume fraction, ℓ/λ is set to an initial guess value and, for each available pair $(\Delta_\infty, h_\infty)$, the corresponding value of λ is calculated by solving numerically Eq. (8). In principle, all λ's thus determined should be the same, if ℓ/λ was chosen correctly, since λ depends only on φ_0. We quantify the dispersion of the λ's by their standard deviation, σ_λ, and repeat this procedure for other guess values of ℓ/λ. Typically, we vary ℓ/λ about the value obtained from the slope of a linear fit of Δ_∞ *vs* h_∞, as suggested by Eq. (9). In all cases, we find that σ_λ varies smoothly with the guess and goes through a clear minimum for some value of ℓ/λ, which is retained as the correct fitting value. The corresponding λ is calculated and finally L is obtained from $\ell/\lambda = L/(L-\lambda)$.
[26] Dowson D *History of tribology* (Longman, New York, 1979).
[27] Ringlein J and Robbins M O 2004 *American Journal of Physics* **72** 884